

RSC Advances



This is an *Accepted Manuscript*, which has been through the Royal Society of Chemistry peer review process and has been accepted for publication.

Accepted Manuscripts are published online shortly after acceptance, before technical editing, formatting and proof reading. Using this free service, authors can make their results available to the community, in citable form, before we publish the edited article. This *Accepted Manuscript* will be replaced by the edited, formatted and paginated article as soon as this is available.

You can find more information about *Accepted Manuscripts* in the [Information for Authors](#).

Please note that technical editing may introduce minor changes to the text and/or graphics, which may alter content. The journal's standard [Terms & Conditions](#) and the [Ethical guidelines](#) still apply. In no event shall the Royal Society of Chemistry be held responsible for any errors or omissions in this *Accepted Manuscript* or any consequences arising from the use of any information it contains.

Seed treatment with iron pyrite (FeS₂) nanoparticles increase the production of spinach

Gaurav Srivastava^{1*}, Chinmaya Kumar Das¹, Anubhav Das¹, Satish Kumar Singh², Manas Roy³, Hansung Kim⁴, Niroj Sethy⁵, Ashok Kumar⁶, Raj Kishore Sharma⁷, Sushil Kumar Singh⁸, Deepu Philip^{9,10}, Mainak Das^{1,10*}

¹ Bioelectricity, Green Energy, Physiology & Sensor Group, Laboratory XII, Department of Biological Sciences and Bioengineering, Indian Institute of Technology Kanpur, Kanpur, Uttar Pradesh, PIN 208016, India

² Institute Nursery, Indian Institute of Technology Kanpur, Kanpur, Uttar Pradesh, PIN 208016, India

³ Department of Chemistry, Lovely Professional University, Phagwara, Punjab, 144411, India

⁴ Department of Chemical & Biomolecular Engineering, Yonsei University, 134 Sinchon-dong, Seodaemon-gu, Seoul, 120-749, South Korea

⁵ Defense Institute of Physiology & Allied Sciences, Defense Research Development Organization, Government of India, Timarpur, Delhi, PIN 110054, India

⁶ Department of Biological Sciences and Bioengineering, Indian Institute of Technology Kanpur, Kanpur, Uttar Pradesh, PIN 208016, India

⁷ Electrochemical Materials Research Group, Division of Physical Chemistry, Department of Chemistry, Delhi University, Delhi, PIN 110007, India

⁸ Functional Materials Division, Solid State Physics Laboratory, Defense Research Development Organization, Government of India, Timarpur, Delhi, PIN 110054, India

⁹ Industrial & Management Engineering, Indian Institute of Technology Kanpur, Kanpur, Uttar Pradesh, PIN 208016, India

¹⁰ Design Program, Indian Institute of Technology Kanpur, Kanpur, Uttar Pradesh, PIN 208016, India

GS and MD are co-corresponding authors. Correspondence and requests for materials should be addressed to

M.D. Email: mainakd@iitk.ac.in

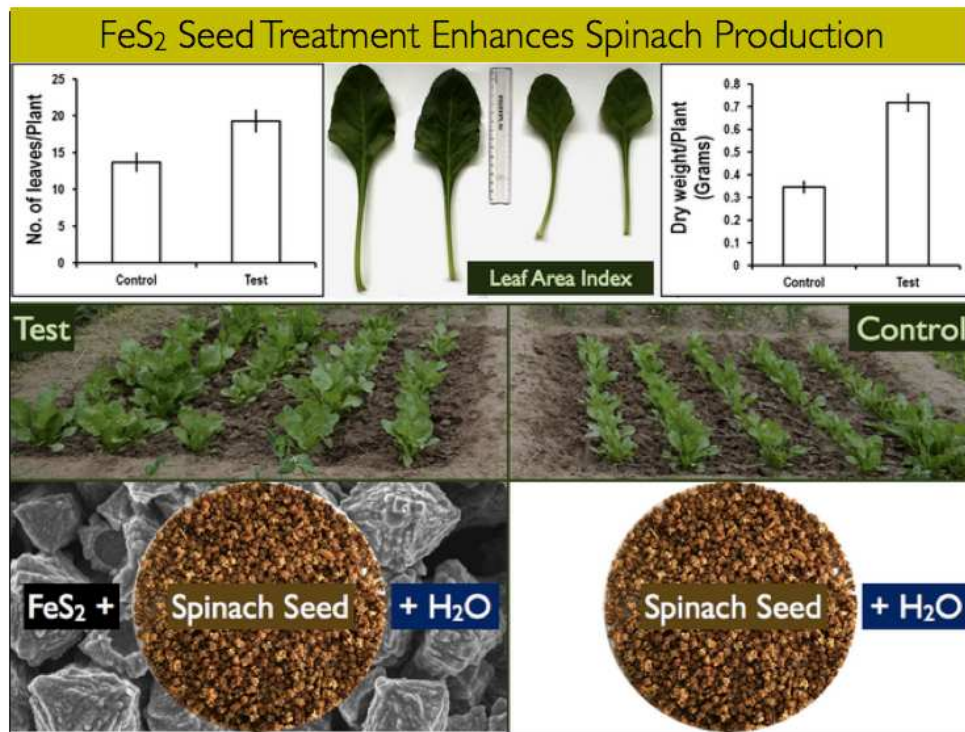


Table of content

Certain nano-materials are known to have plant growth promoting effects, which could find applications in agriculture. We drew inspiration from the nano-factories of deep-sea hydrothermal vents; where iron pyrite nanoparticles serve as fertilizer to sustain chemoautotrophic life forms. We synthesized such iron pyrite nanoparticles in a controlled environment and used them as seed treatment agent (Pro-fertilizer). For us, the term 'pro-fertilizers' represent those materials that when used for seed treatment cause enhanced plant growth with minimum interference to the soil ecosystem. We conducted multi-location field trials on spinach crop, since it is a globally popular crop, consumed as both fresh (salads) and processed food. The spinach seeds were treated for 14 hours in an aqueous suspension of iron pyrite nanoparticle ($\text{FeS}_2 + \text{H}_2\text{O}$) and thereafter directly sown in the field setup for the experiment. The control seeds were only treated in water for the same duration and sown directly in the field. After 50 days, the crop yields from iron-pyrite nanoparticle treated seeds and control seeds were evaluated. The plants developed from iron pyrite nanoparticle treated seeds exhibited significantly broader leaf morphology, larger leaf numbers, increased biomass; along with higher concentration of calcium, manganese and zinc in the leaves when compared to the plants developed from control seeds. We further investigated the possible mechanism resulting in the biomass enhancement following seed-treatment. Our results indicate that there is an enhanced breakdown of stored starch in the iron pyrite treated seeds resulting in significantly better growth. This raises the possibility of developing iron pyrite nanoparticle as a commercial seed-treatment agent (pro-fertilizer) for spinach crop.

Introduction

The projected global population will be approximately nine billion by 2050. To provide healthy nutrition to this projected population; agricultural production will have to be increased by about 60%¹. This increased need mandates the development of innovative and sustainable agricultural strategies. Few such strategies are: application of advance organic fertilizers, reclaiming waste lands, efficient water use, utilizing water bodies for food production, utilizing long forgotten grains¹, effective use of genetically modified crops², synthesizing food in bioreactors, use of nano-materials in veterinary medicine³, integrated pest management⁴ and plant nutrient management^{5, 6}.

Agricultural productivity directly depends on optimal plant nutrient management system. Past few decades of intensive crop production strategies resulted in excessive use of chemical fertilizers, which in turn resulted in deteriorating soil health and increasing water pollution⁷. Strategists, planners and thinkers of modern agricultural practices are pondering on ‘How to reduce the use of chemical fertilizer without compromising on the production?’ In other words, how to develop a sustainable strategy for fertilizers usage.

One approach could be to reduce the size of fertilizers to nano-dimensions so that high surface area to volume ratio can be achieved; where altered surface properties will reduce the dose requirements. This makes nano-fertilizers more advantageous over conventional fertilizers^{5, 6}. In addition, this will reduce the cost of fertilizers and will significantly reduce soil-water pollution. Effectiveness of nano-strategy in developing slow release of fertilizer is reported in case of potash fertilizers⁸ and in urea-modified hydroxyapatite nanoparticles for sustained release of nitrogen in the soil⁹. Carbon nano-structures are also used to increase plant growth^{10, 11}. Most of these nanoparticles that are being tested for their plant growth promoting effects; are of anthropogenic origin (do not exist in nature) and get directly applied in the growth substrate (soil or water). There is no study till date, which attempted to exploit the potency of any kind of nanoparticle as a seed-treatment agent. Although a wide variety of

physical and chemical approaches for seed treatment are documented in the literature; however, the nanomaterial as a seed treatment agent is a comparatively novel approach (Supplementary information: Section S1: Table S1. Detailed list of different seed treatment agents). If such an approach is successful in increasing the yield, then we can reduce the consumption of fertilizers and reap rewards mentioned earlier. We speculate that during the onset of germination, when the seeds are experiencing an extremely fertile metabolic phase, certain nanoparticles may significantly influence the physiology of plant growth; which essentially becomes the premise of this work. In this work, we develop and demonstrate a seed treatment strategy for spinach crop using iron pyrite nanoparticles, which resulted in significantly higher yield.

The most obvious question is ‘why iron pyrite nanoparticles were chosen for our study?’ We drew inspiration from the hydrothermal vents of nature. In late 1970s, several deep-sea expeditions resulted in the discovery of hydrothermal vents and the amazing life forms (giant tubeworms, shrimp, clams and limpets) surrounding these vents. The ecosystem of hydrothermal vent is devoid of sunlight, has high and temperature, and also is rich in iron pyrite nanoparticles and sulfides. These nanoparticles are naturally synthesized in abundance in the nano-factories of the hydrothermal vents. One of the major question arise out of this discovery was ‘how in such an extreme environment, devoid of light, the life form thrives?’ On further probing, it was discovered that the giant tubeworms, which accounts mostly for the very high population in such vents, symbiotically harbors wide range of chemo-autotrophic microbes in their body. The symbiotic microbes are reported to house proteins that are involved in energy coupling by oxidation of the available metal sulfides; primarily FeS_2 ¹². Thus FeS_2 nanoparticle synthesized in the hydrothermal vents act as an energy source for chemoautotrophic life forms¹³⁻¹⁵. It is through this oxidation of sulfides and energy coupling, the higher symbiotic organism i.e. tubeworms obtain its energy for survival. Iron pyrite is also known to be linked with other chemoautotrophic organisms¹⁶ and has great evolutionary significance¹⁷. Researchers also showed interactions between microbes such as *Acidithiobacillus ferrooxidans* and pyrite surface¹⁸. Thus FeS_2 nanoparticle function as a fertilizer for sustaining life forms in deep ocean floor and in oxygen deficient environments. These findings inspired us to look for any relationship between

the FeS₂ and higher autotrophic life forms.

In order to address this problem, we needed pure iron pyrite nanoparticles. Iron pyrite is abundantly present in the nature, but it is contaminated with arsenic¹⁹ and other heavy metals. Therefore, we developed a simple strategy to synthesize pure FeS₂ nanoparticles for our studies. Keeping in mind that in future, we need to reduce the consumption of commercial fertilizers without compromising on the productivity; we decided to use FeS₂ nanoparticles as a seed treatment agent. In one of our recently concluded studies, we have shown that in acute and sterile laboratory conditions; when *Cicer arietinum* seeds are treated with iron pyrite nanoparticles, and grown for 7 days in pure, sterile water; significantly healthy plants with increased dry-weight were observed²⁰. Though our preliminary results were promising; but, from the perspective of a farmer, the major question is: ‘will this novel approach of seed treatment with iron pyrite nano-particles will be effective in the field trials?’ Moreover, ‘will this nano-particle based strategy of crop production is economically effective?’

To address these questions, we evaluated the agricultural production of spinach crop (*Spinacia oleracea*) after seed treatment with FeS₂ nanoparticles. Spinach is popular and global vegetable, which is rich in iron²¹, calcium²² and many vitamins, mainly vitamin A²³. Further, spinach leaf extracts has demonstrated anti-proliferative, anti-aging, anti-inflammatory, and anti-oxidant properties in different experimental models²⁴. We conducted multiple location field trials on this short duration leafy vegetable crop; where harvesting happens after 60 days of sowing. The FeS₂ nanoparticle treated spinach seeds are sown in the fields. After 50 days, we observed that the FeS₂ treated seeds resulted in significantly higher: number of leaves per plant, fresh and dry weight per plant, leaf and leaf area index per plant and higher concentration of calcium, manganese and zinc in the leaves; when compared to control seeds. Further, we proposed a possible mechanism for the observed effects of FeS₂ nanoparticles on the seed physiology. Overall schematic of the study is shown in Figure 1.

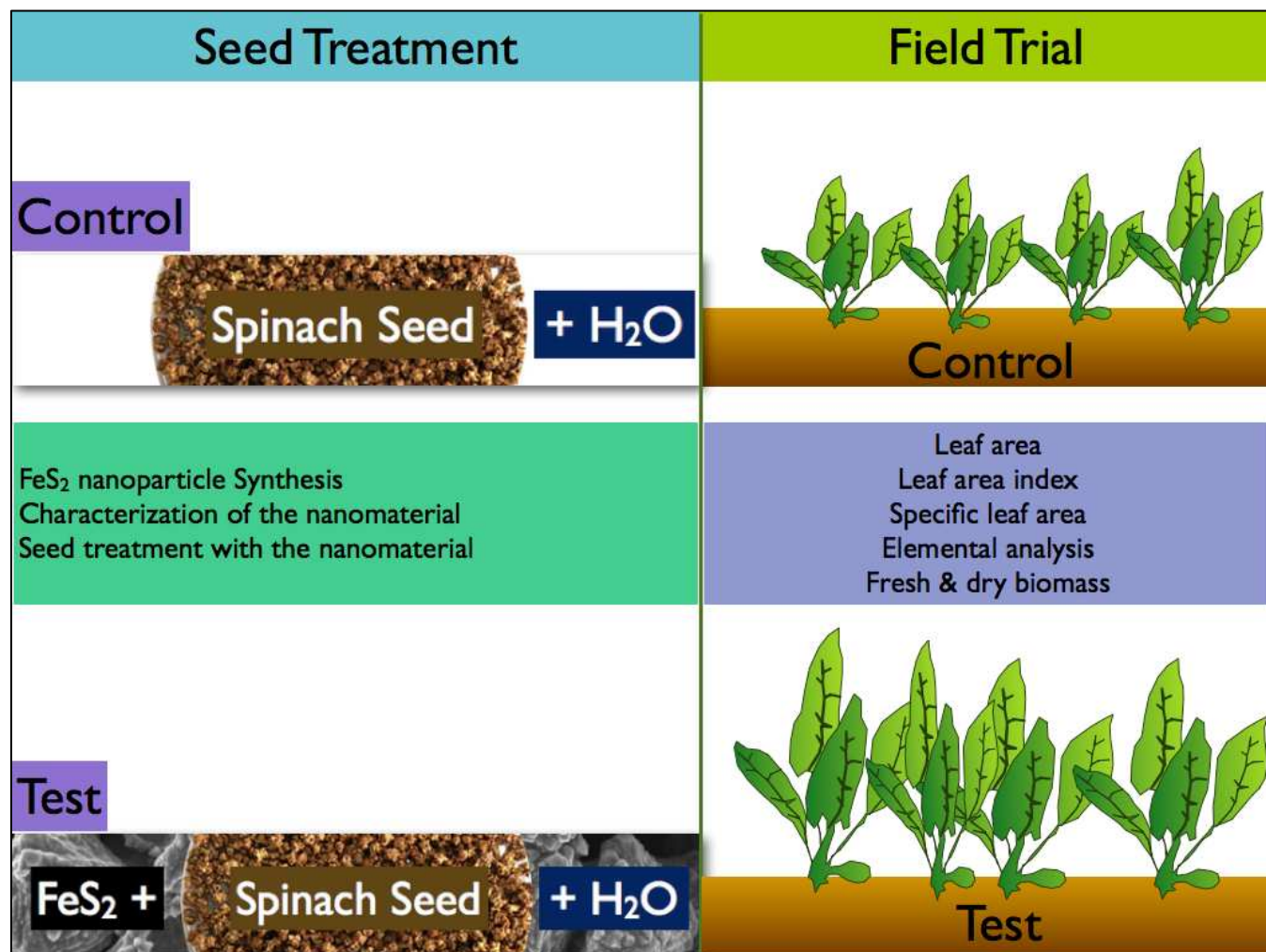


Figure 1. The outline of the study involving synthesis and characterization of nanoparticles, and using them as seed treatment agent, followed by monitoring of the crop yield.

Results and discussion:**Iron pyrite nanoparticle synthesis and characterization:**

We devised a comparatively low temperature synthesis of iron pyrite nanoparticle. The particle size was controlled using tri-sodium citrate (TSC) as a capping agent. The proposed synthesis strategy is a slight modification of our previous work²⁰. The synthesized material was then characterized using X-ray diffraction (XRD) technique and diffraction pattern is shown in figure 2(a). The 2θ peaks at 28.4, 32.8, 36.9, 40.6, 47.3, 56.03 and 58.7 can be indexed to planes (111), (200), (210), (211), (220), (311) and (222), which is in consistency with the iron pyrite structure (JCPDS no. 42-1340); conforming the formation of iron pyrite nanoparticles. The SEM images (figure 2b, c) showed a pitcher like morphology of the particles. The size of the particles ranges from 600-700 nm. The synthesized iron pyrite nanoparticles are of uniform shape, size and morphology.

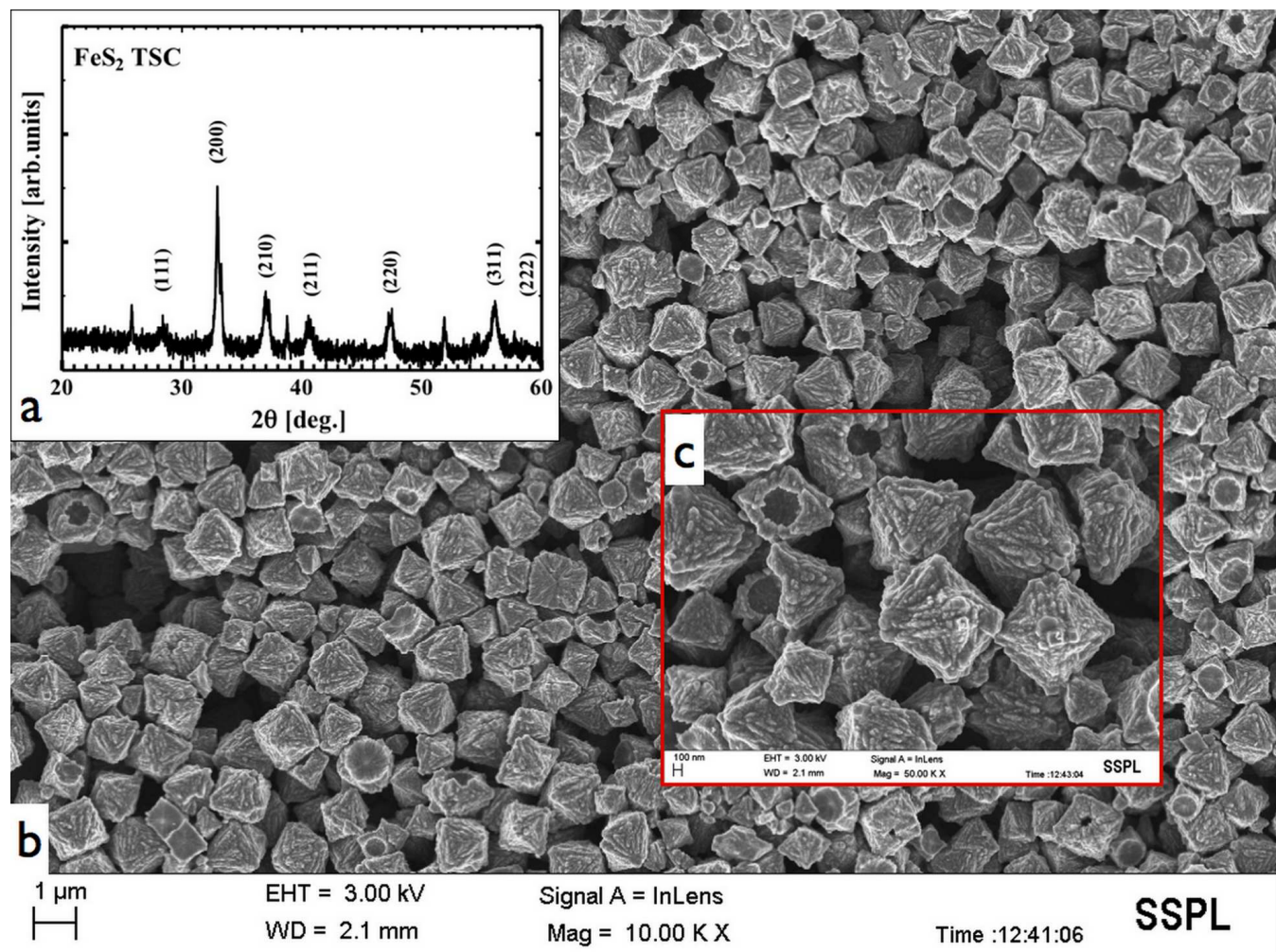


Figure 2. Characterization of synthesized iron pyrite nanoparticle. (a) XRD (b, c) SEM images of the particles showing pitcher like morphology.

XPS analysis of the FeS₂ nanoparticles:

XPS analysis was performed to further verify the composition of the FeS₂ nanoparticles in their native state as well as upon exposure to water. The XPS spectra of both the native samples and the water exposed samples show, two major peaks at 707.5 eV and 720.1 eV due to the Fe2p_{3/2} and Fe2p_{1/2} spin-orbit coupling. The peak at 709.1 eV may be due the defect on the surface of FeS₂. De-convoluted XPS of FeS₂ sample after exposure to oxygen deficient water indicate the formation of FeO, Fe₂O₃, FeOOH and FeSO₄ at binding energy of 710.1 eV, 711.0 eV and 712.0 eV. Further a significantly enhanced signal of Fe₂(SO₄)₃, FeSO₄ and SO₂ was observed in S2p spectra of water exposed sample. Upon exposure to water, noticeable

structural changes were observed in the FeS₂ nanoparticles. In the overall subsequent sections, we have highlighted some of the implications of these reported surface defects on the iron pyrite surface.

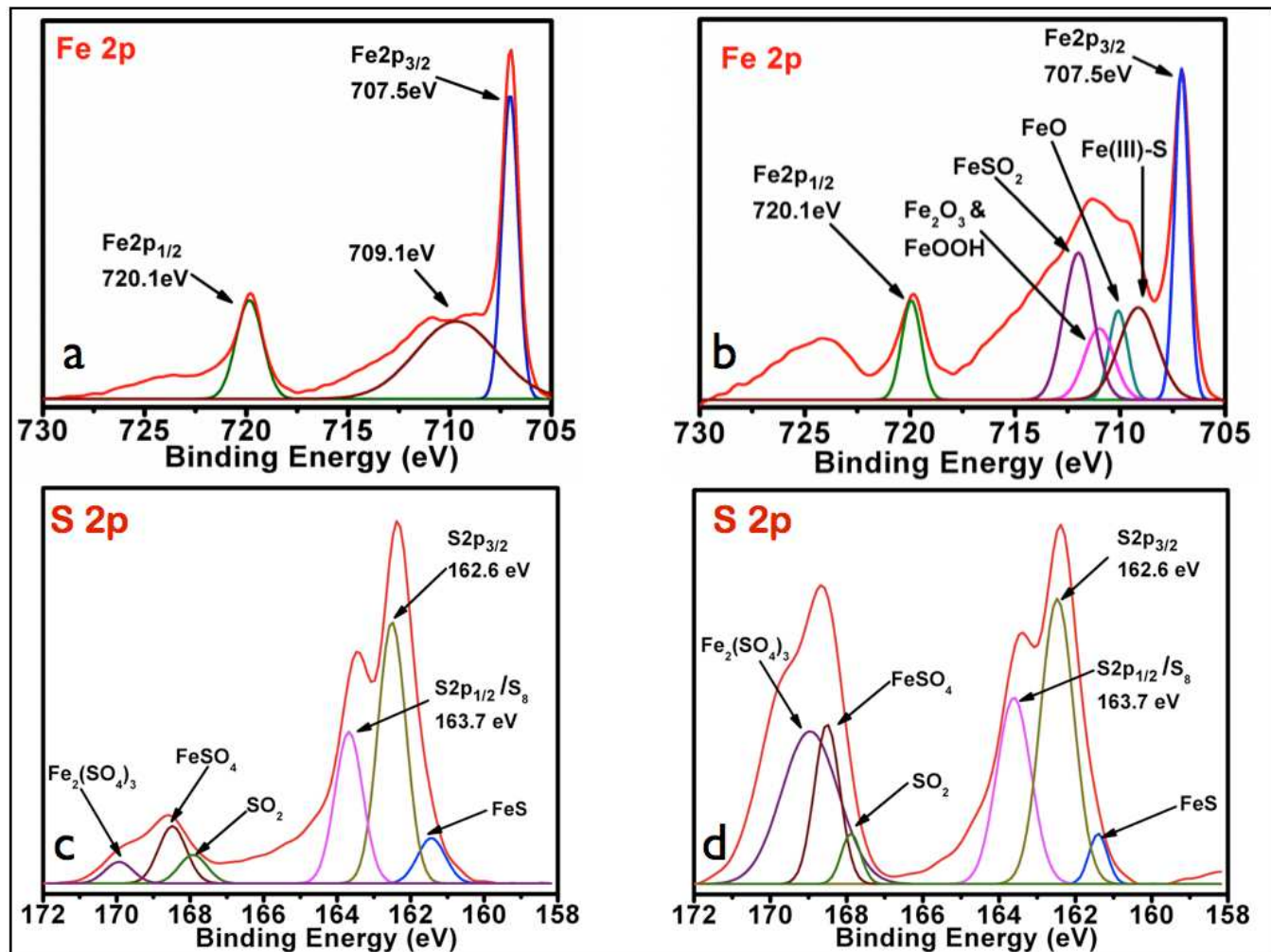


Figure 3. X-ray photoelectron spectra of iron sulphide (FeS₂) nanoparticles. (a) The core Fe2p spectra of the freshly prepared dry FeS₂ sample (b) The Fe2p spectra after exposure to water (c) The core S2p spectra of the freshly prepared dry FeS₂ sample (d) The S2p spectra after exposure to water.

Effect of FeS₂ on the emergence of spinach seed:

We initially investigated the percentage emergence of spinach seeds. In order to compare and quantify the effects of different nanoparticles on the emergence of seeds; we selected three different nanoparticles, viz., iron pyrite (FeS₂), cerium oxide and graphene oxide. Along with this, we quantified the effects of different salts namely Fe²⁺ salt, Cerium salt and charcoal. We

observed significantly higher emergence, when the seeds were treated with FeS₂ (**Supplementary information: The detailed data, synthesis and characterization of the cerium and graphene oxide nanoparticles are given in section S2**). This experiment demonstrated that significantly higher seed emergence is exhibited solely by FeS₂ nanoparticles when compared to other nanoparticles and their corresponding salts. This led us to conduct the field trials using FeS₂ treated spinach seeds.

Plant growth experiments with FeS₂ nanoparticles:

Equal amount of the spinach seeds were randomly divided into 2 groups: (i) control, and (ii) test. The control group seeds were soaked in sterile, double distilled water for 14 hours before sowing; whereas, the test group seeds were soaked in a suspension of double distilled water + FeS₂ particles for 14 hours before sowing them in the field. At the time of harvest, various parameters pertaining to the yield and biomass were calculated. It was observed that control plants had average number of leaves about 13 ± 1 ; whereas, the test plants had average number of leaves at 19 ± 1 (Figure 4a). Specific leaf area was calculated and the data was found corroborating with the data obtained upon measuring the thickness of the leaves (Figure 4b). Also, Figure 4c is the arial view of the field showing that FeS₂ treated seeds resulted in significantly more foliage.

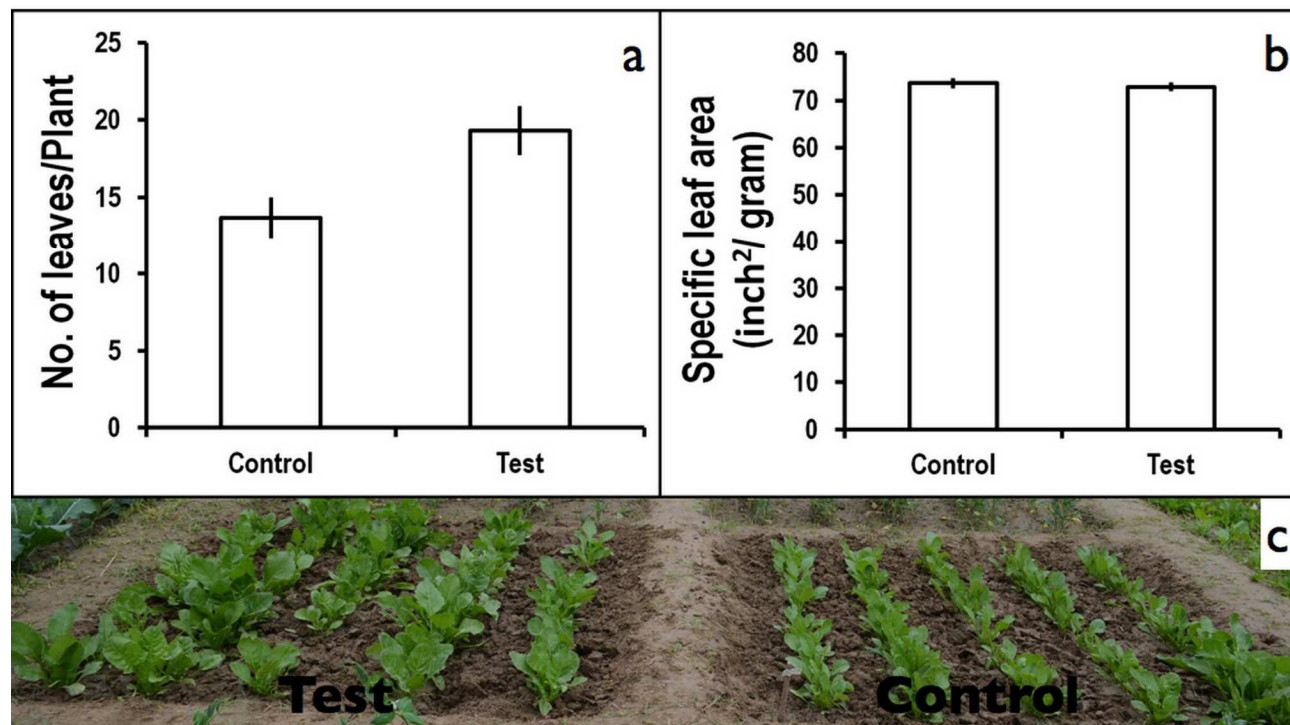


Figure 4. Plant growth parameters: Control versus Test (FeS_2). (a) Number of leaves/Plant: Control: 13 ± 1.0 ; Test: 19 ± 1.0 . (b) Specific leaf area signifies leaf thickness and was found similar for both test and control samples (c) Field photograph taken at day 50 (just before harvesting the crop) depicting that the test group plants have comparatively more foliage as compared to the control plants.

Total leaf area was calculated (Figure 5a) and found to be significantly higher for the test samples. Next, we calculated the 'Leaf Area Index (LAI)', which is a measure of the total photosynthetic area available to the plant. Test samples demonstrated significantly higher 'LAI' with values of 1.53 ± 0.07 , when compared to the control value of 0.94 ± 0.02 (Figure 5b). Representative pictures of the leaves obtained from the test and the control plants are shown in Figure 5c. High leaf area index values also hints at high biomass content of the test samples in comparison to the control.

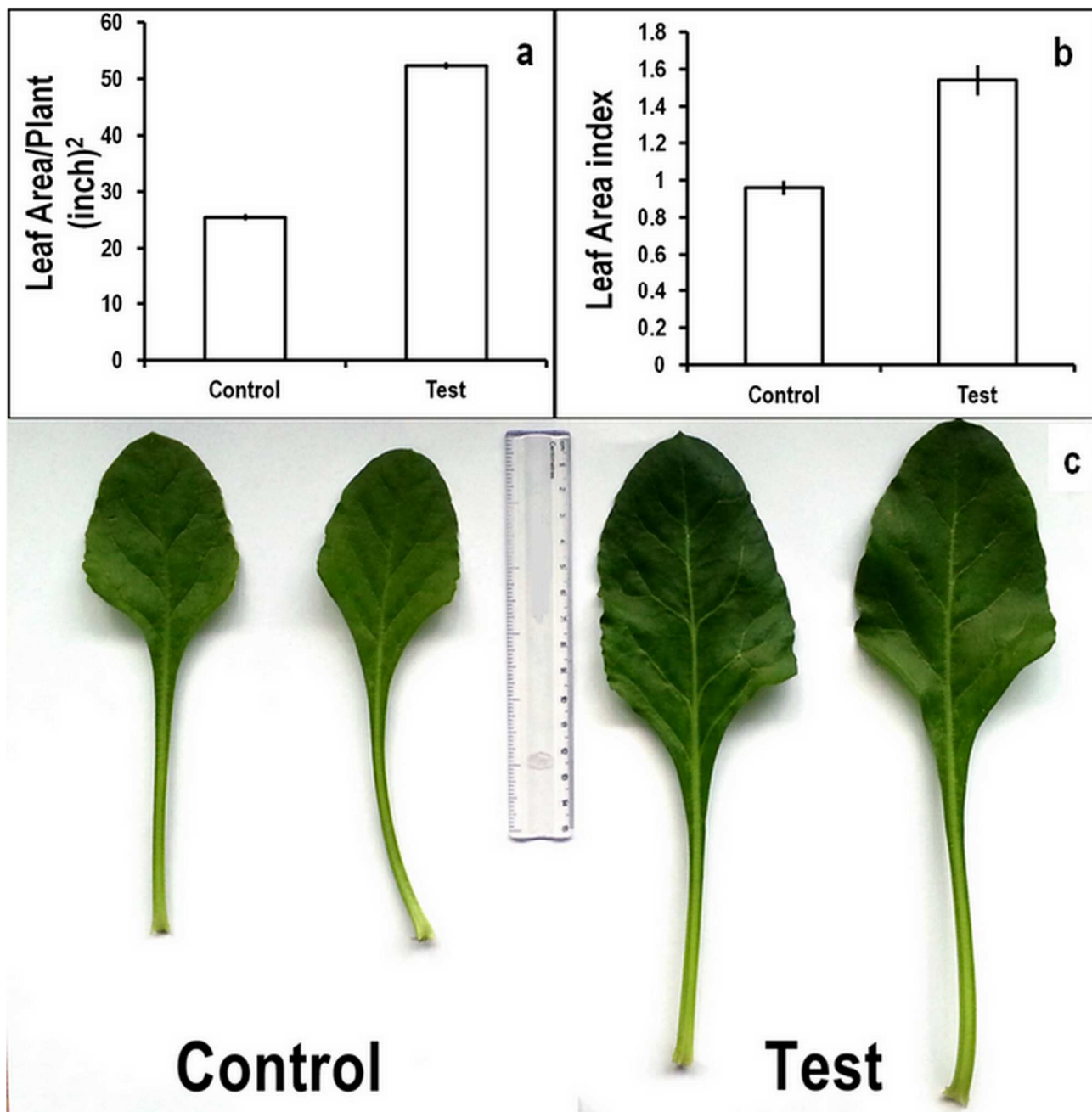


Figure 5. Plant growth parameters: Control versus Test (FeS_2). (a) Leaf area/Plant, showing significant increase in leaf area/test plants (52.4 ± 0.3) as compared to control (25.6 ± 0.2) (b) Leaf area index signifying total photosynthetic area available to plant and high values for test samples (1.5 ± 0.07) can be correlated with high biomass content of pro-fertilized spinach plants in comparison with (0.9 ± 0.02) (c) Comparative photograph of leaves showing larger leaf area in test plants as compared to control plants.

Next we evaluated the fresh and dry weight of control and test plants. Test samples showed tremendous increase in both fresh and dry weight, which is indicative of significant increase in biomass of the test sample upon FeS₂ seed treatment (Figure 6a, b).

Elemental analysis:

The results obtained from spectroscopy showed significant increase in calcium, manganese and zinc in the test samples. However, no significant difference in iron concentration was found between two samples; with mean values 0.1429 ppm with standard error (SE) of 0.0004 for the test, whereas, 0.1406 ppm, SE 0.0017 for the control. Also, values in ppm for calcium, manganese and zinc were 7.621±0.021, 0.6146 ±0.0008 and 1.151±0.003 respectively for test samples and 5.581±0.017, 0.4862±0.0049 and 0.7286±0.0017 respectively for control samples (Figure 6c, d). It should be noted that these values for test samples are significantly higher when compared with control samples. While calcium is involved in structural roles as well as cell signaling²⁵, manganese finds its major role in photosynthesis²⁶. Also, inadequate zinc is known to reduce crop yields and is essential for plant growth²⁷. This significant increase in the concentrations of these important nutrients warrants for further investigations in future. Iron concentration does not show any significant change, which is in accordance with our previous study²⁰. The possible reason why we do not see any significant change in iron concentration is that iron is solely acting as a metal factor in the surface chemical reaction of iron pyrite+water+seed. The mechanism is discussed in the subsequent section.

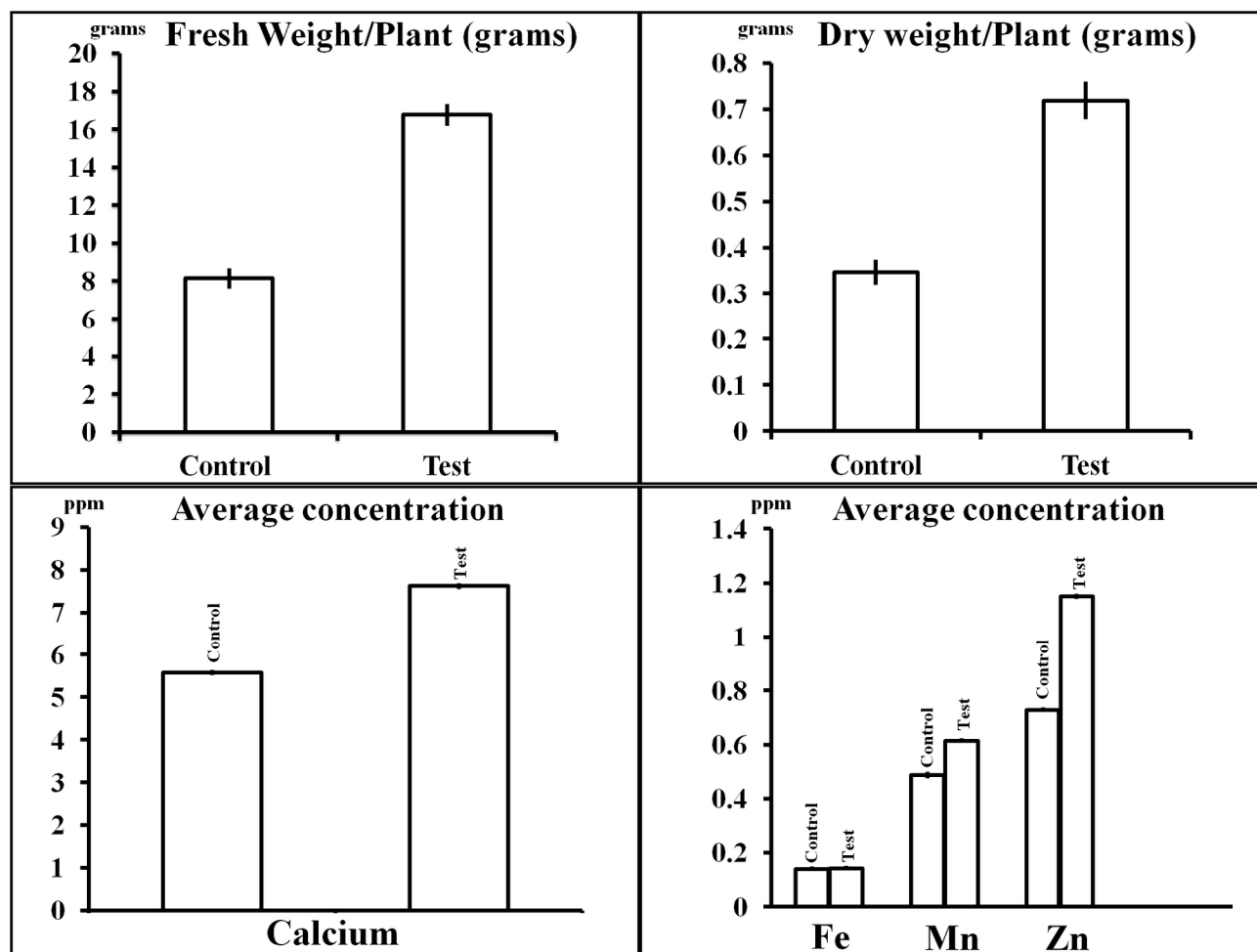


Figure 6. Plant growth parameters: Control versus Test (FeS_2). (a) Fresh weight comparative graph showing significant increase in biomass in test samples (16.7 ± 0.4) as compared to control (8.4 ± 0.4). (b) Dry weight comparative graph corroborating with high biomass content in test plants. Control: 0.3 ± 0.1 ; Test: 0.7 ± 0.1 (c) Calcium concentration in parts per million (ppm). (d) Iron, manganese and Zinc concentration in ppm.

Dissecting the possible mechanism for the observed seed treatment effects:

We attempted to dissect the possible molecular mechanism observed from seed treatment effects through a series of innovative, yet simple experiments. Seeds contain significant amount of stored starch, which is the prime mover for emergence and germination. During germination, seeds derive necessary energy for initial growth by breaking down the stored starch molecules into reducing sugars. This breakdown is enzymatically driven by the family of alpha-amylase enzymes. Thus there is an increase in alpha-amylase activity during germination. The alpha-amylase activity is regulated by

Giberellin, a key plant hormone involve in germination and growth of plants²⁸. This is the most accepted paradigm of seed germination. Figure 7 highlights the key processes of seed germination. We were curious on the role played by FeS₂ particles in this accepted paradigm of seed germination.



Figure 7. The major molecular players involved in the germination of the seeds.

We conducted six sets of experiments, with each replicated six times (n=6) to confirm each of our findings. In the first five cases, the control experiment was seeds treated with double distilled water. For the comparative experiments, the seeds were treated with FeS₂, water, and specific chemicals in certain cases to modulate certain starch breakdown pathways. The experimental layout is given in Figure 8.

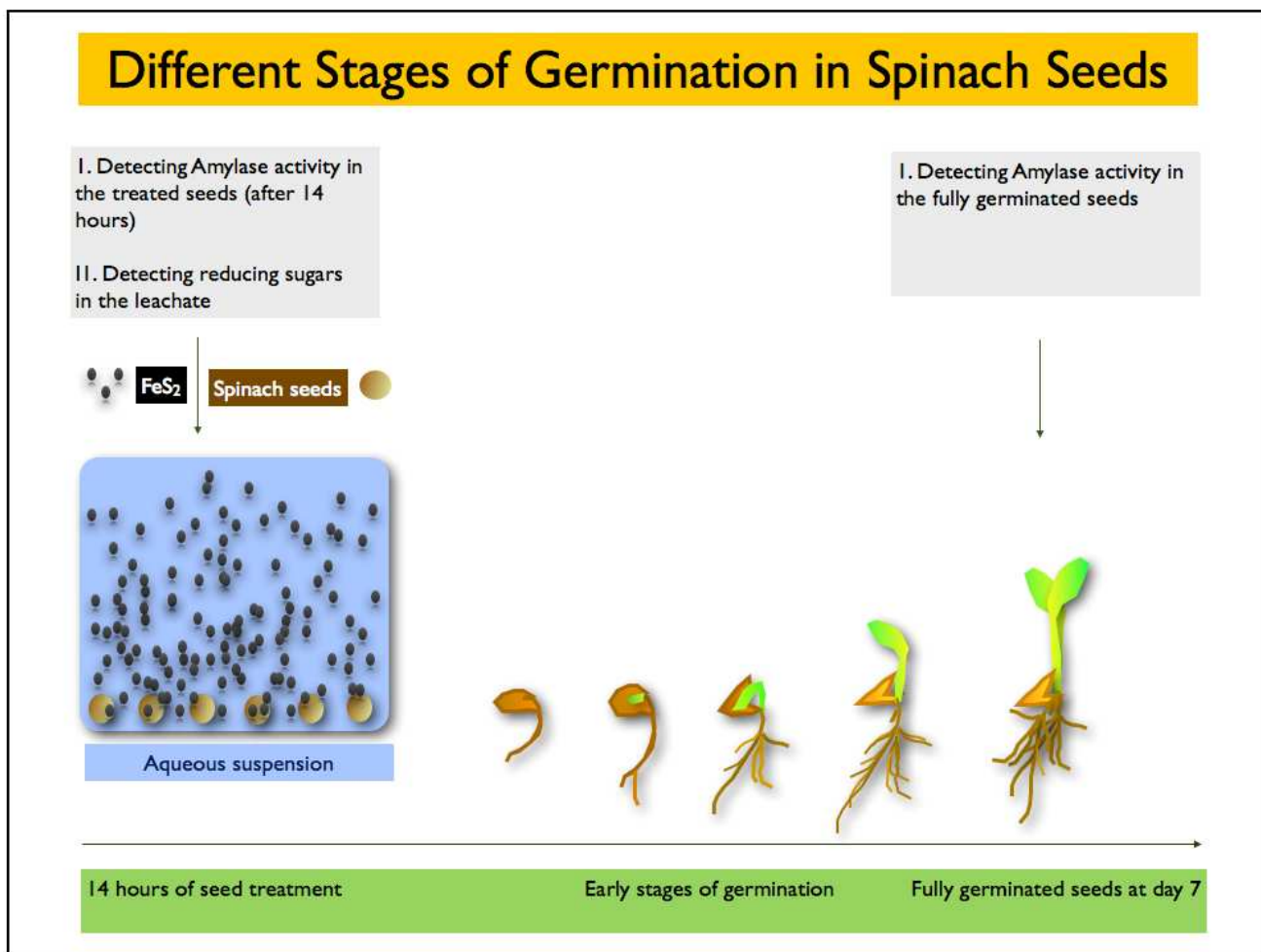


Figure 8. The overall experimental layout to dissect the mechanism of action of FeS₂ on the germination of seed.

In the first experiment, we collected the leachate after 14 hours of seeds treatment from both control and test group. It was analyzed for the presence of reducing sugar. It was found that the test group leachate was 40% more rich in reducing sugars when compared with the control (Figure 9a); allowing us to postulate that higher amylase like activity is promoted by FeS₂ treatment of seeds. Next, we tested for amylase activity in control and treated seeds for durations of 14 hours after treatment and fully germinated seeds at day 7. The amylase activity was found to be 10% and 30% more in both cases respectively (Figure 9b and Figure 9c). The generally accepted fact is that vigorous amylase activity occurs after 72-96 hours of water imbibition during germination, and hence, the higher amylase activity is observed in the later case (Figure 9c). To quantify the influence of FeS₂ on amylase activity, we conducted another set of experiments; where the intrinsic activator of amylase in seeds, viz., Gibberellin was blocked using abscisic acid (ABA). After the treatment with ABA, the amylase activity in the

germinated seeds was significantly reduced as per the accepted theory. However, we observed that fully germinated seeds treated with ABA and FeS₂ demonstrated slight increase (~5%) in the amylase activity at day 7 (Figure 9d). Continuing our investigation, we conducted another set of experiments, where the intrinsic amylase activity was blocked using amylase inhibitor. Interestingly, we found that the fully germinated seeds treated with amylase inhibitor and FeS₂ exhibited ~20% more amylase activity when compared with fully germinated seeds treated with just amylase inhibitor (Figure 9e). These results provoked our curiosity, and we conducted a simple starch breakdown assay in a controlled setting to investigate the capability of FeS₂ alone in breaking down starch molecules in the presence of water. In this experiment, the control was starch plus double distilled water; whereas, the test setup contained starch with double distilled water along with FeS₂. Both setups were kept aside for 14 hours at room temperature; after which the percentage of reducing sugars were estimated in both cases. To our surprise, it was found that the test case demonstrated ~40% more reducing sugar content than the control (Figure 9f).

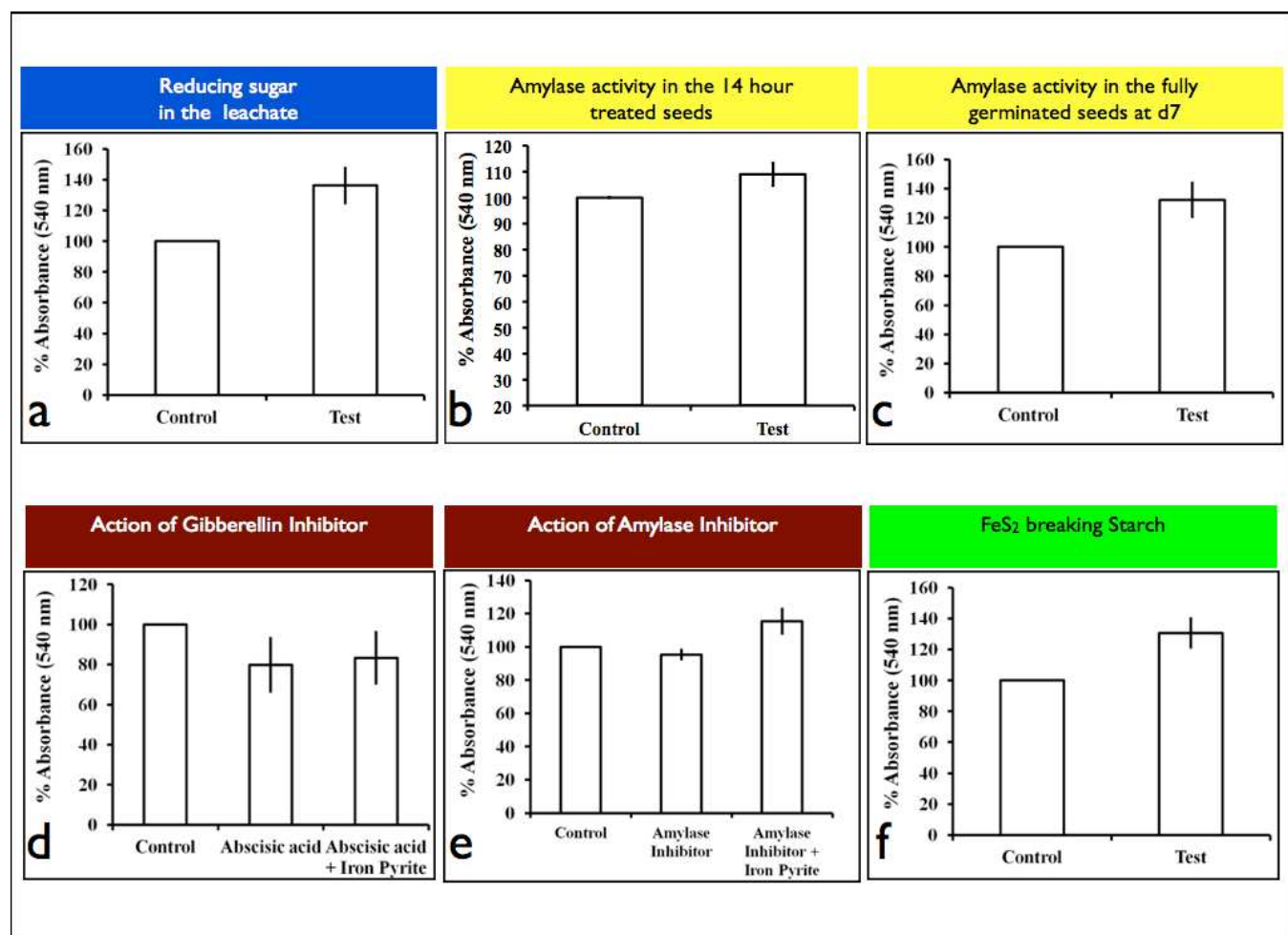


Figure 9. Summary of the experiments to understand the effect of FeS₂ on starch metabolism. All the experiments were repeated 6 times (n=6) and the data was pooled. The results are reported as mean \pm standard error (SE). (a) Total amount of leachate reducing sugars in iron pyrite treated seeds show significant increase (136.23% \pm 11.45) as compared to control seeds' leachate sugars. Values for control have been taken as 100% and the amount of absorbance for test is shown in comparison to the same. (b) Total amount of amylase activity in iron pyrite treated seeds after 14 hours of seed treatment show slight increase (108.85 \pm 4.48) as compared to control seeds' amylase activity. Values for control have been taken as 100% and the amount of absorbance for test is shown in comparison to the same. (c) Total amount of amylase activity in iron pyrite treated seeds after seeding growth (7 days) show significant increase (132.37% \pm 11.57) as compared to control seeds' amylase activity. Values for control have been taken as 100% and the amount of absorbance for test is shown in comparison to the same. (d) Effect of abscisic acid (ABA), a seed dormancy inducer and gibberellin blocker was examined on total amylase activity. A significant decrease in total absorbance was observed (79.86% \pm 13.03) as compared to control. Also incubation with iron pyrite could not bring about a significant positive change (83.33% \pm 12.67). Values for control have been taken as 100% and the amount of absorbance for test is shown in comparison to the same. (e) 5% inhibition in pure amylase activity was observed and thus amylase inhibitor activity was conformed. A marked increase (115.25% \pm 7.33) in the amylase activity was also observed in amylase inhibitor + iron pyrite incubated samples. Values for control have been taken as 100% and the amount of absorbance for test is shown in comparison to the same. (f) Starch breakdown in presence of iron pyrite nanoparticles was seen as there was significant increase (130.62% \pm 9.26) in the absorbance for reducing sugars. Values for control have been taken as 100% and the amount of absorbance for test is shown in comparison to the same.

The hydrolysis of starch to reducing sugars by FeS₂ in the presence of water, and the continuing starch breakdown to reducing sugar even in the presence of amylase inhibitor suggest that FeS₂ alone can breakdown starch in the presence of water. Thus one can say that FeS₂ could mimic the enzymatic activity of amylase enzyme. So the next pertinent question is 'How starch could be hydrolyzed by FeS₂ nanoparticles?' The most plausible reason lies in the intricate surface chemistry of iron pyrite molecule. Iron pyrite surface has 'iron defect' sites²⁹⁻³¹. Further our XPS results highlighted the presence of such surface defects on the iron pyrite nanoparticles (Figure 3). A surface mediated reaction on these defect sites between pyrite and water (either in the absence or presence of oxygen) leads to the production of significant amount of hydrogen peroxide (H₂O₂)²⁹⁻³¹. The amount of H₂O₂ liberated in such reactions is a direct function of defect site density and available surface area of the particles²⁹⁻³¹. So unlike the 'classical Fenton reagent', which is a mixture of hydrogen peroxide and ferrous salts,

there is an *in situ* production of H_2O_2 on the surface of iron pyrite in the presence of water²⁹⁻³¹. This attribute of FeS_2 has led scientists to coin the term the 'pyrite-only Fenton-like' (PF) reagent³². Both Fenton and PF reagent are effective oxidants by virtue of their ability to generate highly reactive hydroxyl radicals. PF has been shown to oxidize wide range of organic compounds including lactate³², carbon tetrachloride³³, chlorinated ethylenes³⁴⁻³⁷, aromatic nitro compounds³⁸ and copper phthalocyanine³⁹. Earlier it has been demonstrated that starch could be hydrolyzed by Fenton reagent⁴⁰. Here we are demonstrating that PF also has the ability to hydrolyze starch. So we could consider iron pyrite nanoparticle system ($\text{FeS}_2 + \text{H}_2\text{O} + \text{Starch}$) as the 'Artificial Enzyme System' mimicking amylase activity in hydrolyzing starch. Thus when seeds are treated with FeS_2 , they have more amylase activity as compared to the control seeds. This enhanced amylase activity and pronounced breakdown of stored starch in the seeds act as a strong growth booster in future development of the plant, as we observe in the field trial.

Next we asked ourselves another question. Is the enhanced biomass of adult plant exclusively due to enhanced amylase activity of the germinated seeds or during that germination phase some other growth promoting pathway might have got triggered? Here we speculate that that H_2O_2 generated by $\text{FeS}_2 + \text{H}_2\text{O} + \text{seed}$ could act as a chemical messenger. Earlier research has reported that H_2O_2 is involved as a secondary messenger in stimulating brassinosteroids mediated CO_2 assimilation, redox signaling and carbohydrate metabolism^{41,42}. Since, FeS_2 can generate hydrogen peroxide in aqueous environment; the brassinosteroid mediated pathway of CO_2 assimilation and carbohydrate metabolism can be enhanced by increased supply of hydrogen peroxide by pyrite. The overall proposed mechanism is outlined in figure 10. Thus, the increase in biomass and plant size upon seed treatment with FeS_2 , can be attributed to the modulation and increased activity of the aforementioned pathway by H_2O_2 generated by FeS_2 .



Figure 10. Proposed outline of the mechanism of action of FeS_2 on spinach seed in enhancing germination and plant growth.

Materials and Methods:

Iron pyrite nanoparticle synthesis and characterization (XRD, SEM, XPS):

Here in this report, we present a low temperature synthesis of FeS₂ nanoparticles using tri-sodium citrate as capping agent. The FeS₂ particles were synthesized by reacting FeCl₃ in an acidic buffer of pH 5.6, along with sodium polysulfide (Na₂S_x) under an inert atmosphere. The basis of this reaction was FeS₂ can be synthesized using polysulfide⁴³. Sodium polysulfide stock was synthesized as described in earlier work. Equal volume (100ml) of Sodium acetate-acetic acid buffer (pH 5.6) and 0.04M FeCl₃ were mixed. Argon was purged for 20 minutes to remove any dissolved oxygen in water, and to prevent any oxidation and thereby maintaining an inert environment. To this solution, 100ml of capping agent i.e. tri-sodium citrate (0.2M) was added and argon purging was done continuously. 15ml of sodium polysulfide was added drop-wise to this solution and a black coloration was observed indicative of FeS formation. Following this continuous stirring and heating in an oil bath at 90-100°C was done for another 4 hours, until black solution turns to grayish in color (Figure 11). The grayish solution obtained was centrifuged and the precipitate was washed as described in earlier work²⁰. Powder X-Ray Diffraction measurements were carried out with a Bruker D8 Advance and a Rigaku miniflex-(II) X-ray diffractometer using monochromatized Cu K α radiation ($\lambda = 1.54056 \text{ \AA}$) at a temperature of 298 K. Scanning electron microscopic (SEM) images were obtained using the SUPRA 40VP field emission scanning electron microscope (Carl Zeiss NTS GmbH, Oberkochen (Germany)). XPS characterization was performed in the PHI Quantera II Scanning XPS microprobe by using a 100 μm x-ray beam at 100 W and at a base pressure of 5×10^{-8} Torr power raster scanning over a $1400 \times 100 \mu\text{m}$ area of the sample.

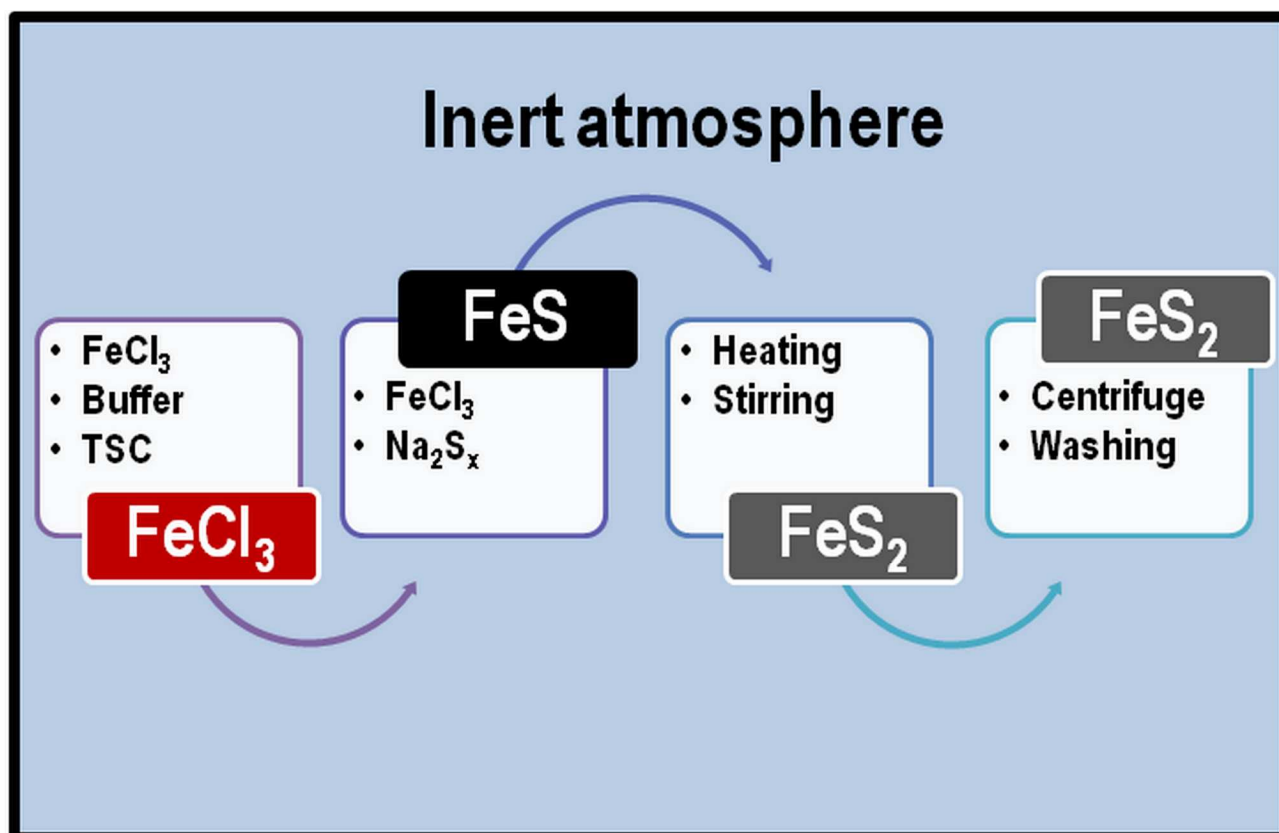


Figure 11. Representative scheme of iron pyrite nanoparticle synthesis. TSC= Tri-sodium citrate; Na_2S_x = sodium polysulfide

Preparation of the plots for conducting field trials:

The plots were randomly chosen in the institute nursery. Each plot, in which trials were conducted, had a dimension of 5 feet x 6 feet. Manual tilling was done and the plots were leveled for proper water distribution. The plots thus prepared were pre-irrigated and left for 3 days for the soil (pH 6.5) to get moistened uniformly. Manual weeding was performed. No insecticide or pesticides were used in these crops. No organic manure or chemical fertilizers were used during the trials.

Plant growth experiments:

Spinach was chosen for plant growth experiments due to its economic importance and high nutritive value. Also spinach has been reported to have high iron concentration. Commercially available spinach seeds were chosen to

ensure the variability in the seeds. The field trials were carried out at three different locations. On each plot of control and test, 1.5 gram healthy spinach seeds were sown. After conducting three different trials (N=3) on randomly selected plots, we observed that both in control and test, around 150 seeds germinated to full grown plants (n=150). The data obtained from three different field trials were pooled to draw the final inferences.

Seed treatment:

The synthesized nanoparticles were used for the seed treatment or pro-fertilization of the spinach seeds. This is a novel approach to study the effectiveness of nanoparticle on plant growth. Three grams of seeds were taken for each trial and three field trials were performed. The seeds were initially treated with 10% sodium hypochlorite solution for 10 minutes to ensure surface sterilization¹⁰ and washed 5 times with de-ionized water to remove any traces of hypochlorite. The seeds were then divided into two equal groups viz. control and test. Control seeds were kept overnight in de-ionized water, while the test seeds were kept in an aqueous suspension of synthesized FeS₂ (80µg/ml of water) in 90mm petri dishes. This dose was optimized in our previous experiments²⁰. The seeds were pretreated for 14 hours and directly sown into the fields.

Evaluating the plant growth parameters:

The following three growth parameters were evaluated: Biomass (fresh weight and dry weight), number of leaves per plant, leaf area per plant, leaf area index and specific leaf area.

1. Biomass and number of leaves per plant: The seeds were allowed to germinate and grow in the fields for 50 days and then harvested manually. Total produce was cleared of any mud attached in the roots by washing in running water and weighed to obtain the fresh weight of the samples. Number of leaves in each plant was counted manually and the samples were further subjected to dry heat in an oven at 75°C for 48 hours. The dried samples were again weighed to get the total dry weight of the produce. This whole procedure was carried out for all the three plots.

2. Leaf area per plant: Ten random fresh leaves were taken from each group i.e. control and test, thickness of each leaf in the middle portion was measured with a micrometer, and no significant difference was found. This data was further corroborated with specific leaf area measurement. One square inch area from 10 random leaves was carefully marked and cut with a scalpel. This area was weighed and total plant area was measured by multiplying the fresh weight of one square inch leaf to the total fresh weight of the produce. The leaf area per plant is calculated by dividing the total leaf area by the total number of plants. Photosynthesis is a function of total leaf area and signifies the amount of biomass produced.

3. Leaf area index: Leaf area index signifies the total photosynthetic area available to the plant and is calculated as the ratio of total leaf area to the total field area. The formula for calculating 'Leaf area index' is [Leaf area index = Total leaf area / Total field area]. Leaf area index was calculated for all three trials and mean was calculated.

4. Specific leaf area: Specific leaf area is calculated as the ratio of leaf area to dry mass. It signifies the thickness of the leaves. The formula for calculating 'Specific leaf area' is [Specific leaf area = Leaf area / Dry mass]. The data obtained was found in corroboration with leaf thickness measurements with the help of micrometer.

Elemental analysis:

Elemental analysis of dried leaf samples was done using inductively coupled plasma spectroscopy (iCAP 6300 ICP Spectrometer, Thermo). Leaf samples were dried in dry heat oven at 75°C for 48 hours, these dried samples were subjected to nitric acid digestion for 2 hours, filtered and the filtrate was used for spectroscopy.

Biochemical assays performed to dissect the mechanism of action of FeS₂ nanoparticles on seed:

1. Leachate sugars: 1 ml of water in which the seeds were soaked overnight was taken in a test tube and 1ml of DNSA (di-nitro salicylic acid) was added along with 1ml of fresh distilled water. The tubes were mixed well and

incubated at 90°C for 10 minutes in a water bath. The solution was allowed to cool down and absorbance was measured at 540nm after 3X dilution.

2. Crude seed extract: Crude seed extract was prepared by grinding the germinated seedlings using a pestle mortar, in 10ml distilled water along with small amount of silicate. The extract thus obtained was filtered and volume was made upto 50ml.

3. Amylase activity test: Amylase test was performed as reported in previous literature with slight modification⁴⁴. 1ml Crude amylase extract was mixed with 1ml citrate buffer (pH 5.6) and incubated at 40°C in a water bath for 10 minutes. To this solution, 2ml of 1% starch solution was added and again kept for incubation at 40°C for 10 minutes. Further to stop the amylase activity, 4ml of 0.4M NaOH was added. 1ml of this final solution was used for DNSA assay for reducing sugars.

4. ABA (Gibberellin inhibitor): Abscisic acid (ABA) is a dormancy inducer and an inhibitor of gibberellin. We used 50 µM of ABA independently and along with FeS₂ during the time of seed treatment. In the control, no ABA was used. ABA was obtained from commercial vendor.

5. Amylase inhibitor extraction from Ragi seeds: Amylase inhibitor extraction was done as described by Kumar et. al. from ragi seeds⁴⁴. 80 gram of seeds were grounded in a pestle mortar to fine powder. 240ml of 0.15M NaCl was added and stirred for 3 hours at room temperature. The slurry obtained was filtered under vacuum. 52 grams of ammonium sulfate was added to 150ml of filtrate and was mixed thoroughly. The solution was allowed to stand overnight at 4°C. This was further centrifuged at 24000g for 20 minutes and the precipitate was dissolved in 50ml distilled water. The solution was properly dialyzed against distilled water. Dialyzed solution was centrifuged for 20 minutes at 24000 g. Further 40 ml of clear supernatant was heated at 70°C for 30 minutes to deactivate amylase and to remove heat labile proteins. The solution was again centrifuged at 24000 g for 20 minutes. The

supernatant was carefully taken and stored at 4°C for further use.

6. Effect of iron pyrite on amylase inhibitor: 2ml of extracted amylase inhibitor was incubated with 100µl of iron pyrite suspension (10mg/ml) for 3hours. This was then centrifuged at 5000 rpm for 20 minutes to get a clear supernatant of amylase inhibitor. Similar procedure was done for control with 100µl distilled water. 1ml of supernatant was carefully taken in a test tube. 1ml amylase (1mg/ml) and 1ml citrate buffer (pH 5.6) were added. This mixture was incubated in a water bath at 40°C for 30 minutes. 2ml of 1% starch solution was added and incubated at same temperature for 10 minutes. This solution was used to carry out DNSA assay for reducing sugars.

7. Iron pyrite and starch incubation: 2ml of 1% starch solution was mixed with 1ml citrate buffer (pH 5.6). 100µl of iron pyrite suspension was added to the test solution and volume of control solution was made up with 100µl distilled water. This was kept overnight (12 hours) in the dark. After incubation the solution was centrifuged at 5000 rpm for 30 minutes and 2ml of the supernatant was carefully taken for DNSA assay.

8. DNSA reagent: 1 gram of di-nitro salicylic acid was added to 50ml water. To this solution 30 grams of sodium-potassium tartrate was added in small amounts. Milky yellow color is observed, which turns to transparent yellow upon addition of 20ml of 2M NaOH. Final volume is made to 100ml and the reagent is kept at 4°C protected from light. We prepared fresh solution for every individual assay.

Conclusion:

We conclude that FeS₂ nanoparticle could function as pro-fertilizer. Simple seed treatment with iron pyrite (FeS₂) nanoparticles increase the production of spinach crop possibly by two different routes. First in the presence of water, it results in *in situ* generation of hydrogen peroxide, thereby breaking down the starch more rapidly. Thus acting as an artificial enzyme mimicking the amylase activity. Second, it acts as a chemical messenger by activating the brassinosteroid pathway, thereby augmenting CO₂ fixation and carbohydrate metabolism. Such innovative seed treatment strategy promises huge prospects in overcoming soil and water pollution and maintaining the soil ecosystem. Such conservative and judicious use of plant growth promoting nanoparticles as seed treatment agent could emerge as a novel strategy in the domain of sustainable agriculture.

Acknowledgment:

We sincerely thank Prof. Tarun Gupta of Department of Civil Engineering, Indian Institute of Technology Kanpur for providing ICP Spectrometer facility. Mr. Rajeev Garg, ‘Superintendent Engineer’ and Head of Institute Works Department (IWD) and Institute Nursery for providing all the logistical supports, labor support for helping in conducting the field trials. Further we appreciate all the help from IIT Kanpur administration for encouraging the field trials.

References:

1. M. Hogenboom, *Science reporter, BBC News*, 2013.
2. S.-E. Jacobsen, M. Sørensen, S. Pedersen and J. Weiner, *Agron. Sustain. Dev.*, 2013, **33**, 651-662.
3. V. P. Chakravarthi and N. Balaji, *Vet World*, 2010, **3**, 477-480.
4. A. Pérez-de-Luque and D. Rubiales, *Pest Management Science*, 2009, **65**, 540-545.
5. M. C. DeRosa, C. Monreal, M. Schnitzer, R. Walsh and Y. Sultan, *Nat Nano*, 2010, **5**, 91-91.
6. R. K. Sastry, H. B. Rashmi, N. H. Rao and S. M. Ilyas, *Technological Forecasting and Social Change*, 2010, **77**, 639-648.
7. X. T. Ju, C. L. Kou, P. Christie, Z. X. Dou and F. S. Zhang, *Environmental Pollution*, 2007, **145**, 497-506.
8. G. K. Ch. V. Subbarao, and D. Sirisha *Internatinal Journal of Applied Science and Engineering.*, 2013, **11**, 25-30.
9. N. Kottegoda, Munaweera, I., Madusanka, N., and Karunaratne, V., *Current Science*, , 2011., **101**, 73-78.
10. S. Tripathi, S. K. Sonkar and S. Sarkar, *Nanoscale*, 2011, **3**, 1176-1181.
11. S. K. Sonkar, M. Roy, D. G. Babar and S. Sarkar, *Nanoscale*, 2012, **4**, 7670-7675.
12. C. R. Fisher and P. Girguis, *Science*, 2007, **315**, 198-199.
13. J. B. Corliss, J. Dymond, L. I. Gordon, J. M. Edmond, R. P. von Herzen, R. D. Ballard, K. Green, D. Williams, A. Bainbridge, K. Crane and T. H. van Andel, *Science*, 1979, **203**, 1073-1083.
14. M. Yucel, A. Gartman, C. S. Chan and G. W. Luther, *Nature Geosci*, 2011, **4**, 367-371.

15. R. A. Zierenberg, M. W. W. Adams and A. J. Arp, *Proceedings of the National Academy of Sciences*, 2000, **97**, 12961-12962.
16. G. Wachtershauser, *Philos Trans R Soc Lond B Biol Sci*, 2006, **361**, 1787-1806; discussion 1806-1788.
17. G. Wächtershäuser, *Systematic and Applied Microbiology*, 1988, **10**, 207-210.
18. H. Tributsch, S. Fiechter, D. Jokisch, J. Rojas-Chapana and K. Ellmer, *Orig Life Evol Biosph*, 2003, **33**, 129-162.
19. J. Matschullat, *Science of The Total Environment*, 2000, **249**, 297-312.
20. G. Srivastava, A. Das, T. S. Kusurkar, M. Roy, S. Airan, R. K. Sharma, S. K. Singh, S. Sarkar and M. Das, *Mater. Express*, 2014, **4**, 23-31.
21. C. H. Schwietzer, *Med. Klin*, 1960, **55**, 1271-5.
22. L. McLaughlin, *J Biol Chem*, 1927, **74**, 455-462.
23. G. Tang, J. Qin, G. G. Dolnikowski, R. M. Russell and M. A. Grusak, *The American Journal of Clinical Nutrition*, 2005, **82**, 821-828.
24. L. Lomnitski, M. Bergman, A. Nyska, V. Ben-Shaul and S. Grossman, *Nutrition and Cancer*, 2003, **46**, 222-231.
25. P. J. White and M. R. Broadley, *Annals of Botany*, 2003, **92**, 487-511.
26. M. R.-D. R. Millaleo, A.G. Ivanov, M.L. Mora, M. Alberdi, *J. Soil Sci. Plant Nutr.*, 2010, **10**, 470-481.
27. M. R. Broadley, P. J. White, J. P. Hammond, I. Zelko and A. Lux, *New Phytologist*, 2007, **173**, 677-702.
28. T. Murata, T. Akazawa, S. Fukuchi, *Plant Physiol.* 1968, **43**, 1899-1905
29. J. M. Guevremont, D. R. Strongin, M. A. A. Schoonen, *Am. Mineralogist*, 1988, **83**, 1246-1255.

30. M. J. Borda, A. R. Elsetinow, M. A. Schoonen, D. R. Strongin, *Astrobiology*, 2001, **1**, 283-288.
31. M. J. Borda, A. R. Elsetinow, D. R. Strongin, M. A. Schoonen, *Geochim. Cosmochim. Acta*, 2003, **67**, 935–939.
32. W. Wang, Y. Qu, B. Yang, X. Liu, W. Su, *Chemosphere*, 2012, **86**, 376-382.
33. M. R. Kriegman-King, M. Reinhard, *Environ. Sci. Technol.* 1994, **28**, 692–700.
34. R. Weerasooriya, B. Dharmasena, *Chemosphere*, 2001, **42**, 389–396.
35. W. Lee, B. Batchelor, *Environ. Sci. Technol.* 2002, **36**, 5147–5154.
36. H. T. Pham, M. Kitsuneduka, J. Hara, K. Suto, C. Inoue, *Environ. Sci. Technol.* 2008 **42**, 7470–7475.
37. H. T. Pham, K. Suto, C. Inoue, *Environ. Sci. Technol.* 2009, **43**, 6744–6749.
38. S. Oh, P. C. Chiu, D. K. Cha, *J. Hazard. Mater.* 2008, **158**, 652–655.
39. C. Gil-Lozano, E. Losa-Adams, A. F.-Davila, L. Gago-Duport, *Beilstein J. Nanotechnol*, 2014, **5**, 855-864.
40. W. R. Brown, *J. Biol. Chem.* 1936, **113**, 417-425.
41. Y. P. Jiang, F. Cheng, Y. H. Zhou, X. J. Xia, W. H. Mao, K. Shi, Z. Chen, J. Q. Yu, *J Zhejiang Univ Sci B*. 2012, **13**, 811-23.
42. G. Barba-Espín, J. A. Hernández, P. Diaz-Vivancos, *Plant Signaling & Behavior*, 2012, **7**, 193–195.
43. G. W. Luther I ii, *Geochimica et Cosmochimica Acta*, 1991, **55**, 2839-2849.

44. A. Kumar, I. Y. Galaev, B. Mattiasson, *Bioseparation*, 1998, **7**, 129-136.